

# Analysis of voltage effect on holographic gratings by modulation transfer function

Rosangela Coromoto Fontanilla-Urdaneta,<sup>1,\*</sup> Arturo Olivares-Pérez,<sup>1,2</sup>  
Israel Fuentes-Tapia,<sup>1</sup> and Mónica Areli Ríos-Velasco<sup>1</sup>

<sup>1</sup>Instituto Nacional de Astrofísica Óptica y Electrónica (INAOE),  
Luis Enrique Erro No. 1 Tonantzintla, Puebla, Mexico

<sup>2</sup>olivares@inaoep.mx

\*Corresponding author: rfontanilla@inaoep.mx

Received 3 November 2010; revised 4 February 2011; accepted 14 February 2011;  
posted 2 March 2011 (Doc. ID 137317); published 22 April 2011

The experimental data allow us to determine the imaging quality of holographic gratings with photo-sensitive film using organic material based on a polyvinyl alcohol matrix doped with potassium dichromate and nickel (II) chloride hexahydrate. The diffraction efficiency is estimated by different spatial frequencies, and the readout image quality is analyzed by the modulation transfer function. The experiment is carried out, with and without voltage application, at different spatial frequencies to obtain the image quality of photosensitive film. © 2011 Optical Society of America

OCIS codes: 050.1950, 090.0090, 090.5694.

## 1. Introduction

Volume-phase holographic gratings (VPHG) have been developed over the past three decades, and they are based on recording interference stationary waves in the volume of the photosensitive coating in order to obtain efficient holograms [1]. Compared with other kinds of storage technologies, volume hologram storage has the advantage of mass capacity, high speed of data transfer, and short time of searching of the address. Thus, volume hologram storage has become the hotspot of superhigh-density storage for several years. The modulation transfer function (MTF) can depict the spatial frequency property of all kinds of imaging systems; it has no relationship to the property and the state of the processed image, and it does not depend on the subjective factor of the observer [2].

Recently, research on holographic recording material by optical recording has been attracting strong interest, and applications on digital recordings,

watermarking, and hologram recording have been continuously conducted [3–5].

In particular, formation of a hologram takes place when the photoinitiator is excited by the illumination pattern, resulting in the formation of radicals. These highly reactive compounds produce a spatially nonuniform polymerization and as result of the concentration gradients produced, monomers diffuse from the dark regions to the neighboring bright regions. Thus, the spatial modulation of the refractive index and its evolution over time is the result of nonuniform polymerization and the diffusion of monomers. The temporal variation of diffraction efficiency depends on the temporal conversion grade of monomer into polymer, so that, depending on the termination process, the response of the diffraction efficiency will be different in function from some physicochemical parameters, such as concentration of photoinitiator, monomer, or intensity [6].

After holographic irradiation of the photopolymer is interrupted at an early stage of the conversion, the thermal postpolymerization enhances the spatial modulation of the segment density between bright and dark areas that goes along with an increase in the modulation of the refractive index and an

improvement in the diffraction efficiency. The key phenomenon is the balance between the chemical initiation of the polymerization and the diffusion of unreacted species from nonlight-struck areas to bright regions of the record [7].

Two regimes of gratings formation for the studied spatial frequency range were distinguished. The nearly linear part corresponds to the polymerization and diffusion of the monomer and methacrylic acid/Zr (O<sup>i</sup>Pr)<sub>4</sub> species during the exposure time, followed by a nonlinear part corresponding to a dark grating formation involving the diffusion mechanism of the two species in the absence of the photoinitiation process. The dynamics of a grating formation in a photopolymer glass with a high refractive index species frequency range of 500–2000 lines/mm has been studied [8].

The addition of poly(acrylic acid) (PAA) in dichromated poly(vinyl alcohol) (PVA) led to the formation of PVA/PAA/ammonium dichromate (ADC) films, which were unstable in the absence of light at room temperature. The reduction of Cr(VI) into Cr(III) provoked chemical and architectural modifications of the polymeric matrix [9].

The spatial resolution, photosensitivity, and diffraction efficiency of the PVA/Acrylamide-based photopolymer system are effectively improved by employing a lower molecular weight binder and increasing the ambient recording temperature [10].

This paper describes the imaging quality of volume holographic gratings on photosensitive organic material film based on a polyvinyl alcohol matrix doped with potassium dichromate and nickel (II) chloride hexahydrate. The diffraction efficiency is determined by different spatial frequencies, and the readout image quality is analyzed by the MTF method. The voltage effect on holographic gratings is also analyzed by MTF.

## 2. Materials and Methods

### A. Materials and Photosensitive Films

The components of photopolymer films are potassium dichromate, nickel (II) chloride hexahydrate, glycerol, and poly(vinyl alcohol) (see Table 1). This hybrid material does not require chemical or thermal processing and is not vulnerable to environmental degradation.

The synthesis of these photopolymer films starts with preparing aqueous solutions for every component. Each solution is stirred and mixed for 45 min to dissolve powder or crystals. In the process, the

solutions are heated for 5 min. The volume ratio of the photosensitive solution is 1:6:1, corresponding to the potassium dichromate (DCP), PVA, and Ni solutions, respectively. This coating solution also contains glycerol (40  $\mu$ l). The mixture is stirred and mixed well to get a homogeneous solution. The dichromated polyvinyl alcohol with nickel (II) chloride hexahydrate (DCPVANi) solution is poured on the clean, leveled substrate. The substrate used in this experiment is glass (Lauka Mexicana S.A. de C.V.). The glass has a thickness of  $1 \pm 0.2$  mm and the area of the plates is 56 mm  $\times$  26 mm. The amount of solution poured on the substrate is 40  $\mu$ l, and it is determined as a function of the desired thickness of the sensitive layer.

The gravity settling method has been adopted to obtain the dried coatings. After deposition of the coating solution on the substrate, a cover should be placed above the plate to prevent dust particles from falling on the film; the drying time for the photosensitive layers is approximately 24 h. The photosensitive composition is sandwiched between glass covers, and between them there are two copper electrodes. The total thickness of the film is 200  $\mu$ m, and it is measured by a Digimatic Model IP65 micrometer (Mitutoyo Corporation, USA).

There is one area for recording the holographic grating with voltage and another area for recording without it. The preparation of the coating solution and films was made at room conditions in the laboratory. The range of room conditions for relative humidity is 42%–62% and for temperature is 18–24  $^{\circ}$ C.

### B. Optical Setup

Figure 1 shows the optical setup for recording the holographic grating and simultaneously measuring the diffraction intensity. The film is exposed to a He–Cd laser, LR (CVI Melles Griot, USA, 50 mW,  $\lambda = 442$  nm). This recording laser beam is moderately attenuated by a filter, F, and is divided into two different intensity beams, IR1 and IR2, by the beam splitter, BS. The intensities are not equal. The mirrors M1 and M2 are used to direct their respective beams on the sample (DCPVANi), creating interference between them. Interfering beams cause modulation of the refractive index. The diffracted light is measured simultaneously during recording by a He–Ne laser, Lr, (CVI Melles Griot, 30 mW,  $\lambda = 632.8$  nm). The intensity of the diffracted beam Ir (+1) is measured at first order by a detector, D. Ir is the light beam from the Lr laser, which impacts on the sample (DCPVANi), where the light that is

Table 1. Components of Photopolymer Material

Component	Chemical Formula	Trademark	Purity	Molecular Weight ( $M_w$ )	Solution Weight Composition
Poly vinyl alcohol (PVA)	(C <sub>2</sub> H <sub>4</sub> O) <sub>x</sub>	Meyer	95.0% [11]	30000 g/ml	7%
Potassium dichromate (DCP)	K <sub>2</sub> Cr <sub>2</sub> O <sub>7</sub>	Baker	99.0%	294.19 g/ml	10%
Nickel (II) chloride hexahydrate (NICHEX)	NiCl <sub>2</sub> • 6H <sub>2</sub> O	Baker	97.0%	237.71 g/ml	10%
Glycerol (Gly)	C <sub>3</sub> H <sub>5</sub> (OH) <sub>3</sub>	Meyer	99.8%	92.10 g/ml	100%

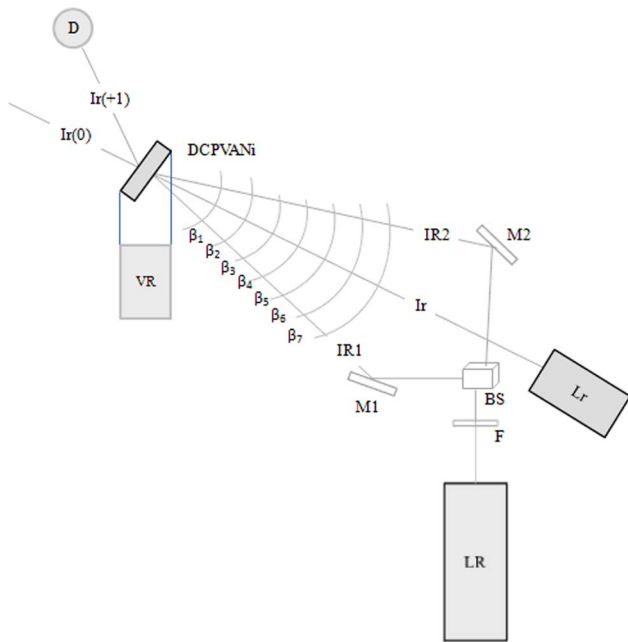


Fig. 1. (Color online) Optical setup for real-time holographic gratings recording by different spatial frequencies.

not diffracted corresponds to  $Ir(0)$ . The diffracted beam is measured during hologram formation as a function of time exposure, but diffraction efficiency is reported as a function of exposure energy. The power source, VR (B&K Precision Corp., USA), of DC voltage is connected to the sample and is regulated until a maximum value of 30 V is reached.

The experiment is carried out with and without voltage application by different spatial frequencies. Table 2 shows the angle of two intersecting recording beams corresponding to each spatial frequency.

### 3. Results

The evolution of diffraction efficiency is determined for diverse spatial frequencies with and without voltage application. The graphics are developed from the estimation of average values for experimental data of diffraction efficiency that corresponds to some sets of recordings for each spatial frequency. The diffraction efficiency is calculated at first order, and its values are normalized and defined by polynomial trend line. The light intensity of the reading beam was  $50 \text{ mW/cm}^2$ . The exposure power average of the recording beam was  $3.4 \text{ mW/cm}^2$ .

Table 2. Angles of Intersecting Recording Beam and Spatial Frequency

	Angle	Spatial Frequency (lines/mm)
$\beta_1$	$24.3^\circ$	666
$\beta_2$	$26.6^\circ$	726
$\beta_3$	$28.1^\circ$	766
$\beta_4$	$30.0^\circ$	816
$\beta_5$	$32.3^\circ$	878
$\beta_6$	$36.1^\circ$	978
$\beta_7$	$40.6^\circ$	1098

The experimental setup described in Fig. 1 shows seven angles that vary from  $\beta_1$  to  $\beta_7$ , and their values depend on the photosensitive plate position and intersecting recording beams. The angle increases as the film approaches the beam splitter. Photosensitive plate films are placed in these seven equally spaced positions, coming toward the beam splitter prism, to the closest position, number seven. Due to the physical size of the mechanical base that supports the photosensitive substrate, these seven measurements are made at constant-sized distances, so that they are obtained with sample nonlinear spatial frequencies and with nonlinear sampling; for this reason, the angles shown in Table 2 are nonlinear, due to the seven positions where samples are taken. This behavior is purely circumstantial, due to the experimental methodology used, but this way of reporting the results does not alter the main context of what we want to describe in this paper.

Only the four more significant curves are reported in this paper to simplify the results presentation. The graphics are made in a logarithmic scale to present the curve more clearly.

#### A. Normalized Diffraction Efficiency without Voltage

The experimental data average of diffraction efficiency without voltage application as a function of exposure energy is illustrated in Fig. 2. The curves of diffraction efficiency are presented by four different spatial frequencies. The maximum diffraction efficiency is achieved when the spatial frequency is 666 lines/mm; the curve reaches two moderate peaks of normalized diffraction efficiency, 0.5 and 1.0, for energies of  $0.5 \text{ J/cm}^2$  and  $8 \text{ J/cm}^2$ , respectively. The curve for 726 lines/mm grows to achieve saturation at an energy of  $4 \text{ J/cm}^2$ , with normalized diffraction efficiency of 0.18.

The curve of diffraction efficiency with a spatial frequency of 816 lines/mm does not achieve a saturation peak. This situation is due to the fact that the experimental process needs more recording energy from the He-Cd laser, but usually the diffraction

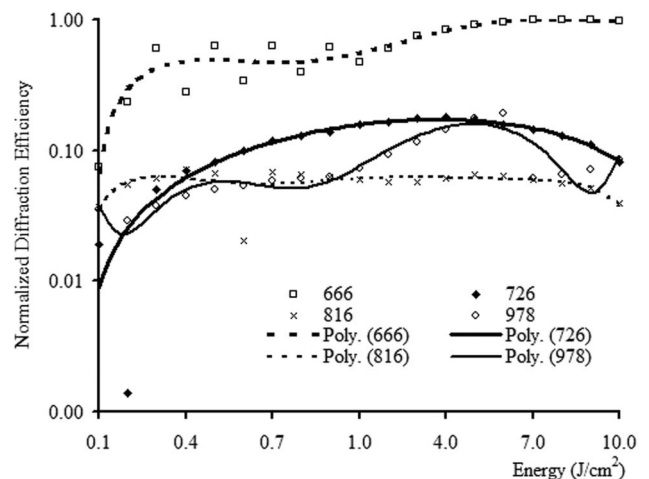


Fig. 2. Evolution of diffraction efficiency without voltage application to different spatial frequencies (logarithmic scale).

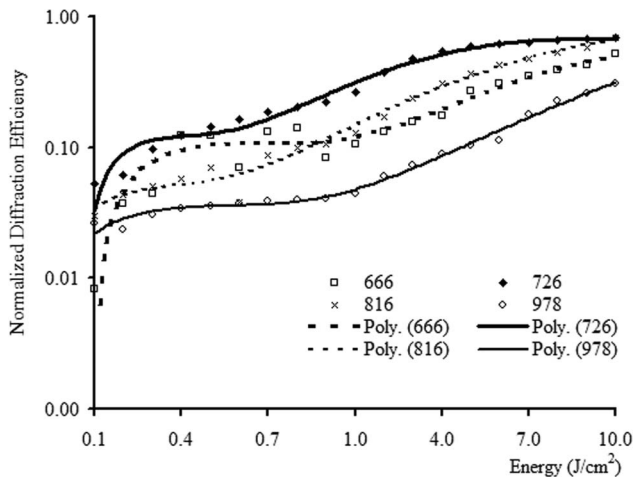


Fig. 3. Evolution of diffraction efficiency with voltage application of 30 V to different spatial frequencies (logarithmic scale).

efficiency rises by voltage application, and it is weak in the absence of voltage. The maximum normalized diffraction efficiency obtained for 978 lines/mm was 0.16 for energy of  $5 \text{ J/cm}^2$ .

Some curves present two peaks: the first one occurs at low energy, and the second takes place when exposure energy is increased. After saturation, the curves start to decrease. The style and response of diffraction efficiency curves depends on the nature of the material.

#### B. Normalized Diffraction Efficiency with Voltage

The curves of normalized diffraction efficiency obtained with 30 V at different spatial frequencies are shown in Fig. 3. The diffraction efficiency curves grow when the exposure energy is increased. The diffraction efficiencies obtained with voltage are higher than those without voltage application for spatial frequencies of 726, 816, and 978 lines/mm. However, the spatial frequency of 666 lines/mm exhibits the opposite results; that is to say, the diffraction efficiencies with voltage are less than without voltage application.

For a spatial frequency of 726 lines/mm, the diffraction efficiency for voltage application increases

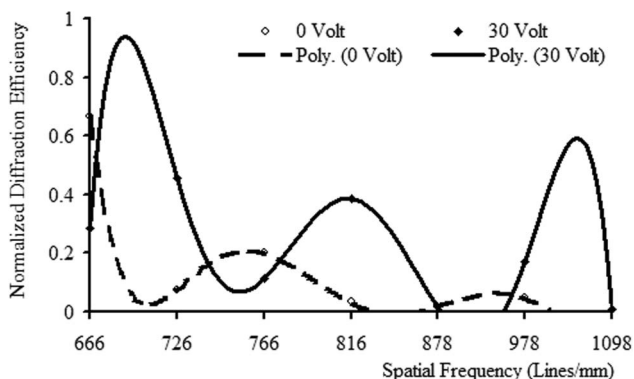


Fig. 4. MTF curve or image quality of holographic gratings on DCPVANI by spatial frequency response. Dashed and solid curves represent 0 and 30 V, respectively.

as soon as exposure energy grows. The maximum normalized diffraction efficiency is 0.7 for energy of  $10 \text{ J/cm}^2$ , but it is necessary to have more energy to perceive an actual saturation. The diffraction efficiency increases quickly by voltage application, and its values are superior to those without voltage. The curves of 666, 816, and 978 lines/mm continue growing, but they do not yet achieve a peak, because there is not enough saturation energy to observe the maximum value of diffraction efficiency.

The curve with voltage of 816 lines/mm trends toward a rapid increase and has more diffraction efficiency than one without voltage; that is to say, the diffraction gratings with voltage have more sensitivity than diffraction gratings without voltage, due to the fact that they produce a significantly faster time of response and rate of photopolymerization. For 978 lines/mm, the evolution of experimental results shows how the diffraction efficiency curve peak is only reached without voltage application, and these values are less than those of the voltage application curve.

#### C. Modulation Transfer Function

The curve of normalized diffraction efficiency as a function of spatial frequency for analyzing the MTF method was developed on photosensitive material. The MTF, or imaging quality of holographic gratings on DCPVANI film by spatial frequency response, is presented by Fig. 4. The best diffraction efficiency values obtained are reported in a range of spatial frequency of 666–726 lines/mm. The photopolymer material has the best image quality for real-time diffraction gratings when the spatial frequency is the lowest of the experimental process. The diffraction efficiency generally increases when the voltage is applied during hologram formation to the photosensitive layer. The contrast and brightness of the image decrease when the spatial frequency increases its value. The response of diffraction efficiency curves depends only on the nature of the material.

#### 4. Conclusions

- Results reported in this manuscript are still preliminary with regard to optimization of the diffraction efficiency capacity and the spatial frequency modulation of the material if the idea is to work as a conventional holographic recording material. This opens the door for future research to optimize these parameters. Nevertheless, there is nothing in the conventional experimental results shown that gives us an idea about the feasibility of this material for duality of behavior: photosensitivity and the ability to conduct electricity. Although the results are modest, it is necessary to emphasize that the potassium dichromate and nickel chloride allow that both dualities persist; it is an important accomplishment owing to the nature of chromium, which generally oxidizes tightly surrounding components. The fact that the nickel chloride is a hexahydrate allows an easy assimilation into the PVA that is used to make

a conductive film, and, in turn with potassium dichromate, a photosensitive film is built.

- The results for a variety of spatial frequencies like the dependence of the diffraction efficiency parameter (MTF) on the applied voltage on holographic gratings, this material becomes a visible image when there is an alteration (modulation) of the material, which is reflected in a increase in the ability to redirect its molecular structure through an affluent of free electrons supplied by the metal salts of nickel chloride. This induces a kind of latent image amplification by free charges, which are reflected as a higher refractive index modulation when it is exposed to the blue light of He—Cd to 442 nm.

- Holographic devices could be developed with this type of material by optimized parameters, and they can become useful in areas such as micro-optoelectromechanical systems and microelectromechanical systems. The fact that diffraction devices can measure information for small electric fields makes this material attractive for technological implementation purposes.

- The voltage application largely increases the diffraction efficiency that is due to the electronic orientation; the flow of free electrons guided along the grooves forms the diffraction gratings. It has an effect of strengthening the modulation of the diffraction gratings due to the free radicals getting excitation with the luminous radiation of the He—Cd laser.

- The image quality of holographic gratings on this photopolymer material is better at low spatial frequency as is observed at the MTF curve; this is due to the natural answer of the space modulation of the material, which is not lineal like many materials.

## References

1. J. P. Laude, *Wavelength Filters in Fiber Optics* (Springer, 2006), pp. 71–123.
2. T. Geng, D.-B. Liu, Z.-Y. Jiang, K. Bi, T. Zhang, and Q. Dai, "Study of the image quality based on MTF in volume hologram storage system," *Proc. SPIE* **6827**, 68271C (2007).
3. H. Yao, M. Huang, Z. Chen, L. Hou, and F. Gan, "Acrylamide-based photopolymer used for holographic recording," *Proc. SPIE* **5060**, 199–202 (2003).
4. S. Blaya, L. Carretero, R. Mallavia, A. Fimia, R. F. Madrigal, M. Ulibarrena, and D. Levy, "Optimization of an acrylamide-based dry film used for holographic recording," *Appl. Opt.* **37**, 7604–7610 (1998).
5. C. Neipp, S. Gallego, M. Ortuño, A. Márquez, A. Beléndez, and I. Pascual, "Characterization of a PVA/acrylamide photopolymer. Influence of a cross-linking monomer in the final characteristics of the hologram," *Opt. Commun.* **224**, 27–34 (2003).
6. S. Blaya, L. Carretero, R. F. Madrigal, M. Ulibarrena, P. Acebal, and A. Fimia, "Photopolymerization model for holographing gratings formation in photopolymers" *Appl. Phys. B* **77**, 639–662 (2003).
7. D. J. Lougnot and C. Turck, "Photopolymers for holographic recording. III. Time modulated illumination and thermal post-effect," *Pure Appl. Opt.* **1**, 269–278 (1992).
8. O. Martínez-Matos, M. L. Calvo, J. A. Rodrigo, P. Cheben, and F. Del Monte, "Diffusion study in tailored gratings recorded in photopolymer glass with high refractive index species," *Appl. Phys. Lett.* **91**, 141115 (2007).
9. A. Barichard, Y. Israël, and A. Rivaton, "Why does poly(acrylic acid) addition improve the quality of holograms recorded in dichromated poly(vinyl alcohol)?," *Eur. Polym. J.* **45**, 1791–1797 (2009).
10. J. Zhu, G. Wang, Y. Hao, B. Xie, and A. Y. S. Cheng, "Highly sensitive and spatially resolved polyvinyl alcohol/acrylamide photopolymer for real-time holographic applications," *Opt. Express* **18**, 18106–18112 (2010).
11. S. K. Saxena, Chemical and Technical Assessment 61st JECFA (FAO, 2004).